International Journal of Mathematical, Engineering and Management Sciences
Vol. 9, No. 5, 1185-1197, 2024
https://doi.org/10.33889/IJMEMS.2024.9.5.062

Ram Arti Publishers

Creep Stress Analysis of Transversely Isotropic Rotating Disc Composed of Piezoelectric Material

Vikash Ghlawat
Department of Mathematics, School of Basic Sciences and Research,
Sharda University, Greater Noida, Uttar Pradesh, India.
E-mail: 2020400516.vikash@dr.sharda.ac.in

Richa Sharma
Department of Mathematics,
Jaypee Institute of Information Technology, Sector 62, Noida, Uttar Pradesh, India.
Corresponding author: richa.sharma@mail.jiit.ac.in

Khursheed Alam
Department of Mathematics, School of Basic Sciences and Research,
Sharda University, Greater Noida, Uttar Pradesh, India.
E-mail: khursheed.alam@sharda.ac.in

(Received on December 22, 2023; Revised on April 17, 2024 & May 14, 2024; Accepted on May 31, 2024)

Abstract
If a crystal undergoes mechanical stress, then an electrical potential is developed across its sides; this phenomenon is called piezoelectricity, or the piezoelectric effect. Piezoelectric materials include quartz, zinc oxide (ZnO), lead zirconate titanate (PZT4), and Rochelle salt. There are numerous uses for piezoelectricity in signal and electrical transducers. In this work, transitional and creep stresses are evaluated in a thin disc made up of piezoelectric transversely isotropic solids subjected to rotation. The mathematical expressions of stress components are computed for the rotating disc by using Seth's transition theory considering the rotation effect in circular disc. The electric displacement relations and various stress components are computed using Hooke's Law. A non-homogeneous differential equation is obtained by using mathematical relations and the equilibrium equation. The theoretical solution of the differential equation is obtained under specified boundary conditions. Creep stresses are studied for the considered material. The obtained results are shown graphically, analyzed numerically, and concluded with a discussion of the results for transversely isotropic piezoelectric materials such as $BaTiO_3$ and PZT-4, among others. On the basis of all the numerical discussions and graphs, it is concluded that discs composed of transversely isotropic piezoelectric (PZT4 and $BaTiO_3$) materials are more stable than discs composed of transversely isotropic (magnesium and beryl).

Key words- Transversely isotropic, Piezoelectric, Rotating disc, Transition theory.

List of Symbols

e_{rr}	Radial strain	θ	temperature
$e_{\theta\theta}$	Circumferential strain	r	Function of x and y
u, v, w	Displacement components	β	Function of r only
ω	Angular velocity	ρ	Density
t_{rr}	radial stress	d	Constant
$t_{\theta\theta}$	circumferential stress	A, B	Constants of integration
c_{11}, c_{12}, c_{13} and c_{66}	are material constants	D	Constant
e_{11}, e_{12}, e_{13}	are piezoelectric coefficients		

1. Introduction

In the present era, smart materials are of economic and scientific importance in engineering and scientific research. Smart materials are defined as materials having properties that can be significantly changed by the applications of external stimuli, such as stress, variation in temperature, moisture, pH, electric, or magnetic fields. Some of the popular examples of smart materials are piezoelectric material, shape memory alloys, shape memory polymers, pH-sensitive polymers, magneto-caloric material, pyroelectric material, and thermo-piezoelectric material. The internal generation of an electric current as a result of mechanical force applications is known as direct piezoelectric material. The materials that exhibit the piezoelectric effect are known as piezoelectric materials. Piezoelectric materials are widely used in various sensing devices, such as waves, shock control devices, MEMS devices, navigation, medical instruments, household kitchen appliances, and smart structures. In solving the problem of piezoelectricity, it becomes evident to include the temperature effect to discuss the temperature range in which the piezoelectric effect works. Creep stress analysis is a branch of material science and engineering that focuses on understanding the deformation of materials over long periods of time under constant stress or load. Unlike traditional elastic behavior, where materials return to their original shape once the load is removed, materials subjected to creep exhibit time-dependent and permanent deformation even under constant stress at elevated temperatures.

The theories for electrical, thermal, and mechanical coupling have been developed by various authors. Altenbach and Skrzypek (1999) provide insights into the phenomenon of creep, which refers to the tendency of materials to deform over time under a constant load or stress. The damage mechanisms in materials and structures are given in their book Creep and Damage in Materials and Structures. Hoseini et al. (2011) described a new analytical solution for creep stresses in rotating cylindrical shells under internal and external pressure using Nortan's law. Mindlin (974) study of the propagation of Rayleigh waves in a homogeneous isotropic piezo-electric microstretch-thermoelastic solid half-space. Chandrasekharaiah (1988) analyzed the linear thermos elasticity theory in the case of piezoelectric media. Tauchert (1992) examined the thermal elastic behavior of a piezoelectric plate of crystal. Singh and Gupta (2009) presented an analysis of the steady state creep in an Al-SiCP composite cylinder subjected to internal pressure and concluded that by reducing SiCP size, increasing SiCP concentration, and lowering the operating temperature, the tangential and radial strain rates in the cylinder decreased significantly. Penny and Marriott (1995) determined the effects of creep in the cylinder using a method that was exactly the same as an equivalent elastic one. Rimrott (1959) discussed the creep stresses in thick-walled tubes under the influence of pressure on the inner surface by considering large strains. Betton (2005) analyzed the creep stresses in thick-walled shells exposed to pressure on the inner surface. Using big strain theory, Bhatnagar and Arya (1974) investigated the effect of anisotropy on creep stresses in spherical, thick-walled containers under internal pressure. Bhatnagar and Gupta (1969) performed the creep analysis of an orthotropic cylinder and concluded that creep anisotropy significantly affects the behavior of the cylinder. The exposure of high temperatures to solid properties is a major concern for designers. This effect of temperature depends on several aspects, including the material, loading conditions, and state of stress. In addition to these effects, an increase in temperatures results in creep or "time-flow" deformations in materials. Creep is expressed as the time-dependent deformation generated in solids which are subjected to stress.

Many researchers, for example Temesgen et al. (2020), discovered creep deformation in a revolving disc that is transversely isotropic, has a variable density shaft, and is exposed to a heat gradient. Zhou et al. (2024) used a double Legendre polynomial quadrature-free approach, and the results showed that the frequency-radius product tended to stabilize as the gradient index increased and as the radius-thickness ratio climbed. Bagheri et al. (2015) investigated the dynamic behavior of an orthotropic substrate that was weakened by changing fissures and strengthened by a non-homogenous covering. Primarily, an incomplete

orthotropic functionally graded coating screw dislocation solution is obtained for the orthotropic strip. Fartash et al. (2019) examined the dynamic behavior of two bonded dissimilar piezoelectric layers containing multiple interfacial cracks subjected to electro-mechanical impact loading.

For evaluating the creep and elastic plastic stresses in different structures, many authors have applied the concepts of transition theory (Borah, 1971). Sharma and Yadav (2019) determined the numerical solution for the elastic-plastic thermal stresses in the thin rotating FGM disk with exponentially varying thickness and density and came to the conclusion that the FGM disc is safe for design. Sharma et al. (2018) have analyzed the creep stresses in a transversely isotropic circular cylinder under pressure on the inner surface and found that a non-homogeneous cylinder is a better choice. Kumar and Ailwalia (2019) studied a dynamic problem in a piezo-electric microstretch thermoelastic medium under a laser heat source, and the results show that the coupled tangential stress values are significantly influenced by the laser heat source. Sharma et al. (2017) evaluated the creep stresses in a rotating disc. Sharma & Sahni (2020) analyze the creep stresses in a thin rotating disc composed of piezoelectric material and observe that stresses increase significantly with angular velocity and pressure. Sharma (2019) employed transition theory to carry out a pressure-dependent stress analysis on a functionally graded annular disk whose thickness is variable exponentially and found that variable thickness and non-homogeneity have a major impact on the circumferential stresses. Sharma (2023) illustrated the analytic solution for thermal stresses in a thin, rotating, transversely isotropic disc composed of variable thicknesses and densities of piezoelectric material. The research's parameters can be utilized to create radar antennae, pressure sensors, and a variety of other machines, structures, and devices for use in engineering applications. Singh et al. (2020) used a threshold stress-based law to assess creep stress in rotating composite discs with the same volume and average thickness. It was discovered that a disc with a hyperbolic thickness profile offers the best creep response.

Yang et al. (2021) investigated the stratified structural sandstone's creep behavior and crack evolution under segmental constant load and established a foundation for determining the stratified rock mass's creep behavior under various load situations. Saadatfar et al. (2024) assessed the deformation and stress of a functionally graded piezoelectric rotating disk that was subjected to mechanical and thermomechanical loads, including heat transfer via radiation and convection. The findings demonstrate that the spinning FGPM disc's responses are significantly influenced by solar radiation, the convection boundary, the thickness function, and the inhomogeneity index. Thakur and Sethi (2020) examined stress and creep deformation in a transversely distributed material disk under a rigid shaft and found that for a transversely isotropic disk, strain rates reach their greatest value at the inner surface. Chand et al. (2023) examined the stresses in an annular isotropic disc under internal pressure and discovered that, in contrast to incompressible material, hoop stress is maximum close to the disc's outer surface for compressible material. Matvienko et al. (2023) examined the plastic deformation of a revolving annular disk made of alloys toughened by dispersion to aluminum using optical microscopy techniques and mechanical tension testing. Es-Saheb and Fouad (2023) examined the creep behavior in a rotating thick-walled cylinder composed of Al-SiCP composite subjected to constant load and internal and external pressures using the finite element method, and it was observed that with an increase in the internal pressure in the cylinder, there is a corresponding increase in strain rates. All the above-mentioned authors evaluated the elastic plastic and creep stresses in discs or cylinders composed of different types of piezoelectric materials, but creep stresses in rotating discs composed of transversely isotropic piezoelectric materials under pressure and temperature were not discussed by any of them. This is the novelty of this problem.

In this paper, creep stresses are computed in a rotating disc composed of transversely isotropic piezoelectric material under the influence of pressure and temperature on the inner surface. The methodology of

transition theory is applied to the presented problem. The purpose of using this theory is to explain the nonlinearity of the transition state, which was not considered in the classical theory of mechanics. The resulting quantities are depicted graphically to explore the effect of piezoelectric parameters, internal pressure, and temperature on the rotating disc.

2. Mathematical Formulation

Consider a thin rotating disc of and internal and external radii of a and b, with an angular velocity ω. A thin disc is assumed as we are discussing the state of plane stress i.e. $T_{zz} = 0$. The displacements in cylindrical polar co-ordinates are as follows (Borah, 1971)

$$u = r\,(1-\beta); v = 0;\ w = dz \tag{1}$$

where, d is constant and β is a function of $r = \sqrt{x^2 + y^2}$.

The radial, circumferential and longitudinal components of strain are as follows:

$$e_{rr} = \frac{1}{n}[1-(r\beta+\beta)^n], e_{\theta\theta} = \frac{1}{n}[1-\beta^n], e_{zz} = \frac{1}{n}[1-(1-d)^n] \tag{2}$$

According to Hooke's law, stress-strain relations for transversely isotropic piezoelectric materials are

$$t_{rr} = c_{11}e_{rr} + (c_{11} - 2c_{66})e_{\theta\theta} + c_{13}e_{zz} - e_{11}E_r - \beta_1\theta$$

$$t_{\theta\theta} = (c_{11} - 2c_{66})e_{rr} + c_{11}e_{\theta\theta} + c_{13}e_{zz} - e_{12}E_r - \beta_2\theta$$

$$t_{zz} = t_{zr} = t_{r\theta} = t_{\theta z} = 0 \tag{3}$$

where, t_{rr} = radial stress and $t_{\theta\theta}$ = circumferential stress, c_{11}, c_{12}, c_{13} and c_{66} are material constants; e_{11}, e_{12}, e_{13} are piezoelectric coefficients. $\beta_1 = \alpha_1 c_{11} + 2\alpha_2 c_{12}$; $\beta_2 = \alpha_1 c_{12} + 2\alpha_2(c_{22} + c_{33})$, α_2 is the quantity perpendicular to the symmetry axis, and α_1 is the linear thermal expansion coefficient.

$\theta = \frac{\theta_0 \log(r/b)}{log(a/b)}$, θ_0 is constant.

The electric displacement equation is

$$D_r = e_{11}e_{rr} + e_{12}e_{\theta\theta} + e_{13}e_{zz} + \eta_{11}E_r,$$
$$D_\theta = D_z = 0 \tag{4}$$

where, η_{11} is dielectric constant.

The electrical displacement must satisfy Maxwell's equation, which requires that the divergence of the electrical displacement vanishes at any point within the medium.

$\frac{\partial D_r}{\partial r} + \frac{D_r}{r} = 0$, From this equation of free charge and Equation (4) we get,

$$D_r = \frac{C_1}{r} = \frac{1}{r},\ E_r = \frac{1}{\eta_{11}}\left[\frac{1}{r} - e_{11}e_{rr} - e_{12}e_{\theta\theta}\right] \tag{5}$$

The equation of equilibrium is given by

$$\frac{d}{dr}(rt_{rr}) - t_{\theta\theta} + \rho w^2 r^2 = 0 \tag{6}$$

Using Equation (3)-(5) in equation of equilibrium (6) we get

$$\frac{d}{dr}(rt_{rr}) - t_{\theta\theta} + \rho\omega^2 r^2 = r(r\beta' + \beta)^{n-1}\frac{d}{dr}(r\beta' + \beta)\left\{-c_{11} - \frac{e_{11}^2}{\eta_{11}}\right\} + \frac{1}{n}\{1 - (r\beta' + \beta)^n\}\left\{c_{11} + \frac{e_{11}^2}{\eta_{11}}\right\} - (c_{11} - 2c_{66}) + \frac{e_{11}e_{12}}{\eta_{11}} + r\beta^{n-1}\frac{d\beta}{dr}\left\{(c_{11} - 2c_{66}) + \frac{e_{11}e_{12}}{\eta_{11}}\right\} + \frac{1}{n}(1 - \beta^n)\left\{(c_{11} - 2c_{66}) + \frac{e_{11}e_{12}}{\eta_{11}} - c_{11} - \frac{e_{12}^2}{\eta_{11}}\right\} + \frac{e_{12}}{\eta_{11}}.\frac{1}{r} - \beta_1 r\frac{d\theta}{dr} + \rho\omega^2 r^2 \quad (7)$$

Putting $r\beta' = \beta P$ in Equation (7), the following non-linear equation in β is obtained

$$-\left[c_{11}\beta^{n+1}P(1+P)^{n-1} + \beta^{n+1}P(1+P)^{n-1}\frac{e_{11}^2}{\eta_{11}}\right]\frac{dP}{d\beta} = [1 - \beta^n(1+P)^n]\left[\frac{e_{11}}{n\eta_{11}}\{e_{11} - e_{12}\} + 2c_{66}\right] + P\beta^n\left\{c_{11} - 2c_{66} + \frac{e_{11}e_{12}}{\eta_{11}}\right\} + \frac{1}{n}(1 - \beta^n)\left\{-2c_{66} + \frac{e_{12}}{\eta_{11}}(e_{11} - e_{12})\right\} + \beta^n P(1+P)\left\{c_{11} + \frac{e_{11}^2}{\eta_{11}}\right\} + \frac{1}{r}\frac{e_{12}}{\eta_{11}} - \frac{\beta_1}{r}\frac{\theta_0}{log(a/b)} + \rho\omega^2 r^2 \quad (8)$$

3. Transition from Elastic State to Creep State

According to Seth's transition theory, the conversion from an elastic to a creep state under external loading occurs through a transition state. The transition can take place through the principal stresses T_{rr}, $T_{\theta\theta}$ or the principal stress difference $T_{rr} - T_{\theta\theta}$ becoming critical. It has been assumed in transition theory that (Borah, 1971) the asymptotic solution through the principal stresses leads from an elastic state to a creep state at transition points $P \to \pm 1$. For evaluation of creep stresses, the transition function is taken as

$$R = t_{rr} - t_{\theta\theta} \quad (9)$$

$$R = c_{11}\frac{1}{n}[1 - \beta^n(1+P)^n] + (c_{11} - 2c_{66})\frac{1}{n}[1 - \beta^n] + c_{13}\frac{1}{n}[1 - (1-d)^n] - \frac{e_{11}}{\eta_{11}}\left(\frac{1}{r} - e_{11}e_{rr} - e_{12}e_{\theta\theta}\right) - \beta_1\frac{\theta_0\log\left(\frac{r}{b}\right)}{log(a/b)} - \left[\frac{1}{n}(c_{11} - 2c_{66})\frac{1}{n}[1 - \beta^n(1+P)^n] + \frac{c_{11}}{n}(1-\beta)^n + \frac{c_{13}}{n}(1 - (1-d)^n) - \frac{e_{12}}{\eta_{11}}\left(\frac{1}{r} - e_{11}e_{rr} - e_{12}e_{\theta\theta}\right) - \beta_2\frac{\theta_0\log\left(\frac{r}{b}\right)}{log(a/b)}\right] \quad (10)$$

Taking logarithmic differentiation of Equation (10), we get

$$\frac{d}{dr}(log\,R) = \frac{\frac{2c_{66}\eta_{11} + e_{11}^2 - e_{12}e_{11}}{r(e_{11}\eta_{11} + e_{11}^2)}\left\{(-c_{11} + 2c_{66})\frac{\beta^n}{r} - \frac{e_{11}}{\eta_{11}r^2} - \frac{e_{11}e_{12}}{r}\beta^n - \beta_2\frac{\theta_0\log\left(\frac{r}{b}\right)}{log(a/b)} + \rho\omega^2 r\right\} + \frac{2c_{66}}{r}\beta^n + \frac{e_{11} - e_{12}}{\eta_{11}r^2} - \frac{e_{12}}{r}\beta^n - (\beta_1 - \beta_2)\frac{\theta_0}{rlog(r/b)}}{(c_{11} - 2c_{66})\frac{1}{n}[1 - \beta^n] - \frac{e_{11}}{\eta_{11}r} + \frac{e_{11}e_{12}}{\eta_{11}n}[1 - \beta^n] - \beta_1\frac{\theta_0\log\left(\frac{r}{b}\right)}{log(a/b)}} \quad (11)$$

Taking the value of $\beta = \frac{D}{r}$ as $P \to -1$, where, D is constant in Equation (11), we get

$$\frac{d}{dr}(log\,R) = \frac{\frac{2c_{66}\eta_{11} + e_{11}^2 - e_{12}e_{11}}{r(e_{11}\eta_{11} + e_{11}^2)}\left\{\begin{matrix}(-c_{11} + 2c_{66})\frac{\left(\frac{D}{r}\right)^n}{r} - \frac{e_{11}}{\eta_{11}r^2} - \frac{e_{11}e_{12}}{r}\left(\frac{D}{r}\right)^n \\ -\beta_2\frac{\theta_0\log\left(\frac{r}{b}\right)}{log(a/b)} + \rho\omega^2 r\end{matrix}\right\} + \frac{2c_{66}}{r}(D/r)^n + \frac{e_{11} - e_{12}}{\eta_{11}r^2} - \frac{e_{12}}{r}(D/r)^n - (\beta_1 - \beta_2)\frac{\theta_0}{rlog(r/b)}}{(c_{11} - 2c_{66})\frac{1}{n}\left[1 - \left(\frac{D}{r}\right)^n\right] - \frac{e_{11}}{\eta_{11}r} + \frac{e_{11}e_{12}}{\eta_{11}n}\left[1 - \left(\frac{D}{r}\right)^n\right] - \beta_1\frac{\theta_0\log\left(\frac{r}{b}\right)}{log(a/b)}}$$

$$\frac{d}{dr}logR = G;\ logR = \int G\,dr + logA$$

$$R = Ae^{\int G dr} = AH; \text{ where, } H = e^{\int G dr} \quad (12)$$

where,

$$G=\frac{\frac{2c_{66}\eta_{11}+e_{11}^2-e_{12}e_{11}}{r(e_{11}\eta_{11}+e_{11}^2)}\left\{(-c_{11}+2c_{66})\frac{(D/r)^n}{r}-\frac{e_{11}}{\eta_{11}r^2}-\frac{e_{11}e_{12}}{r}(D/r)^n-\beta_2\frac{\theta_0\log\left(\frac{r}{b}\right)}{log(a/b)}+\rho\omega^2 r\right\}}{+\frac{2c_{66}}{r}(D/r)^n+\frac{e_{11}-e_{12}}{\eta_{11}r^2}-\frac{e_{12}}{r}(D/r)^n-(\beta_1-\beta_2)\frac{\theta_0}{rlog(r/b)}}{(c_{11}-2c_{66})\frac{1}{n}[1-(D/r)^n]-\frac{e_{11}}{\eta_{11}r}+\frac{e_{11}e_{12}}{\eta_{11}n}[1-(D/r)^n]-\beta_1\frac{\theta_0\log\left(\frac{r}{b}\right)}{log(a/b)}}.$$

The boundary conditions that need to be applied at the inner and outer surfaces of the disc are assumed to be

$$t_{rr}=-p \quad at \quad r=a \ and \ t_{rr}=0 \quad at \quad r=b \tag{13}$$

As equation of equilibrium is given by

$$\frac{d}{dr}(t_{rr})-\frac{t_{rr}-t_{\theta\theta}}{r}+\rho w^2 r=0 \tag{14}$$

Putting the value from Equation (12) in (14) and integrating we have

$$t_{rr}=\int\frac{AH}{r}dr-\frac{\rho w^2 r^2}{2}+B \tag{15}$$

From Equations (9), (12) and (15) we have

$$t_{\theta\theta}=\int\frac{AH}{r}dr-\frac{\rho w^2 r^2}{2}-AH+B \tag{16}$$

Apply boundary condition $t_{rr}=-p \quad at \quad r=a$,we get

$$\left[A\int\frac{H}{r}dr\right]_{r=a}-\frac{\rho w^2 a^2}{2}+B=-p \tag{17}$$

Apply boundary condition $t_{rr}=0 \quad at \quad r=b$, we get

$$0=\left[A\int\frac{H}{r}dr\right]_{r=b}-\frac{\rho w^2 b^2}{2}+B \tag{18}$$

Using Equation (17) and (18), we obtain

$$p+\frac{\rho w^2(a^2-b^2)}{2}=A\left[\left[\int\frac{H}{r}dr\right]_{r=a}-\left[\int\frac{H}{r}dr\right]_{r=b}\right] \tag{19}$$

Now we have found the values of $A \ and \ B$,

$$A=\frac{p+\frac{\rho w^2(a^2-b^2)}{2}}{\int_a^b\frac{H}{R}dR},$$

$$B=\frac{\rho w^2 b^2}{2}-\frac{p+\frac{\rho w^2(a^2-b^2)}{2}}{\left[\int\frac{H}{r}dr\right]_{r=a}-\left[\int\frac{H}{r}dr\right]_{r=b}}\left[\int\frac{H}{r}dr\right]_{r=b} \tag{20}$$

The components in non-dimensional form are assumed as

$$R=\frac{r}{b},R_0=\frac{a}{b},\sigma_r=\frac{t_{rr}}{p},\sigma_\theta=\frac{t_{\theta\theta}}{p},\sigma_\theta=\frac{t_{\theta\theta}}{p},\Omega=\frac{\rho\omega^2 b^2}{p} \tag{21}$$

Stresses in non-dimension form are as follows:

$$\sigma_r=\frac{t_{rr}}{p}=\int\frac{A_1H_1}{R}dR-\frac{\Omega}{2R^2}+B_1,$$

$$\sigma_\theta = \frac{t_{\theta\theta}}{p} = \int \frac{A_1 H_1}{R} dR - \frac{\Omega}{2R^2} - A_1 H_1 + B_1 \tag{22}$$

where, $A_1 = \frac{1+\frac{\Omega\left(R_0{}^2-1\right)}{2}}{\int_{R_0}^{1} \frac{H_1}{R} dR}$, $B_1 = \frac{\Omega}{2R^2} - \frac{1+\frac{\Omega\left(R_0{}^2-1\right)}{2}}{\int_{R_0}^{1} \frac{H_1}{R} dR} \int_R^1 \frac{H_1}{R} dR$ and

$$\frac{2c_{66}\eta_{11}+e_{11}^2-e_{12}e_{11}}{bR(e_{11}\eta_{11}+e_{11}^2)} \left\{ \begin{matrix} (-c_{11}+2c_{66})\frac{\left(\frac{D}{bR}\right)^n}{bR} - \frac{e_{11}}{\eta_{11}(bR)^2} - \frac{e_{11}e_{12}}{bR}\left(\frac{D}{bR}\right)^n \\ -\beta_2 \frac{\theta_0 \log R}{log R_0} + \frac{\Omega b^2}{R^2} \end{matrix} \right\}$$

$$H_1 = \frac{+\frac{2c_{66}}{bR}(D/bR)^n + \frac{e_{11}-e_{12}}{\eta_{11}(bR)^2} - \frac{e_{12}}{r}(D/bR)^n - (\beta_1-\beta_2)\frac{\theta_0}{bRlog(R_0)}}{\frac{(c_{11}-2c_{66})}{n}[1-(D/bR)^n] - \frac{e_{11}}{\eta_{11}bR} + \frac{e_{11}e_{12}}{\eta_{11}n}[1-(D/bR)^n] - \beta_1 \frac{\theta_0 \log R}{log R_0}}.$$

4. Numerical Discussion

The standard values of all the material constants for the considered materials are used in **Table 1**. To illustrate the impact of angular velocity and temperature on creep stress distributions, the values of the parameters used in this study were selected arbitrarily. All the graphs are drawn using Mathematica software. **Figures 1 to 18** represent the creep stresses in the case of transversely isotropic (Magnesium and Beryl) and transversely isotropic piezoelectric (PZT4 and $BaTiO_3$) materials for linear $(n = 1)$ and nonlinear $(n = 0.7, 0.5)$ measures for different values of temperature $(\theta = 0.5, 0.3)$ and angular velocities $(\Omega = 5,10,20)$ with different radii ratios $R = \frac{r}{b}$.

Table 1. Values of material constants of transversely isotropic and transversely isotropic piezoelectric materials.

Material property	Material constants	$BaTiO_3$ (Piezoelectric)	PZT-4 (Piezoelectric)	Magnesium (Transversely isotropic)	Beryl (Transversely isotropic)
		10^9 N/m^2	C/m^2		
Elastic constants	C_{11}	275.1	139.0	5.97	2.746
	C_{13}, C_{66}	151.6, 81	74.3, 30.6	2.17, 1.675	0.67, 0.883
Piezoelectric Constants	(e_{11}, e_{12})	21.3, 3.7	12.7, 15.1	NA	NA
Dielectric constant	η_{11}	16.9	6.5	NA	NA

Followings are the graphs of creep stresses with different radii ratios.

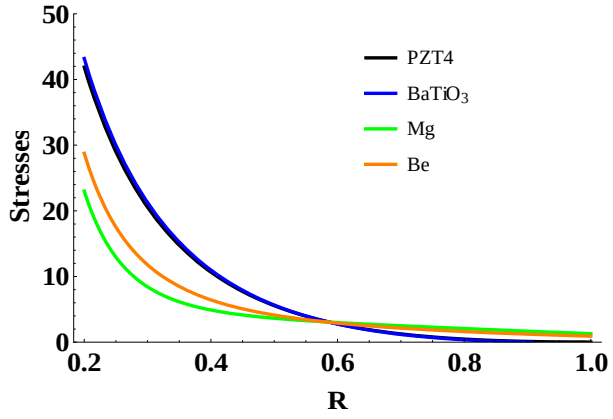

Figure 1. Graphs of creep stresses with $\theta = 0.5$, $\Omega = 5$ and measure n =1.

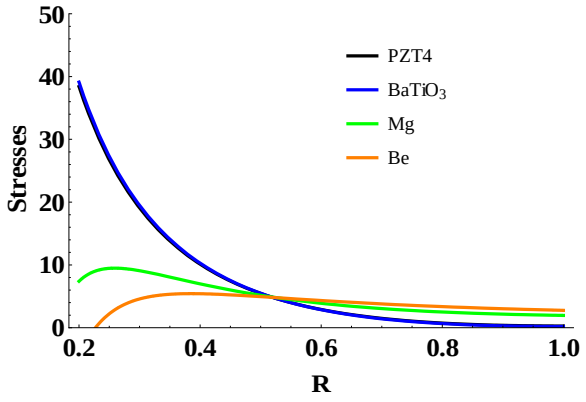

Figure 2. Graphs of creep stresses with θ = 0.5, Ω = 5 and measures n = 0.7.

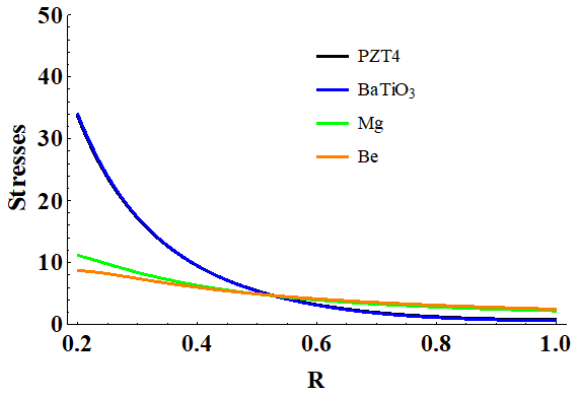

Figure 3. Graphs of creep stresses with $\theta = 0.5$, $\Omega = 5$ and measure n = 0.5.

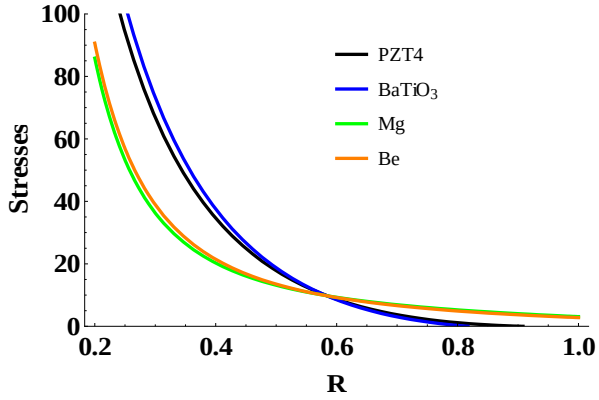

Figure 4. Graphs of creep stresses with $\theta = 0.5$, $\Omega = 10$and measure n = 1.

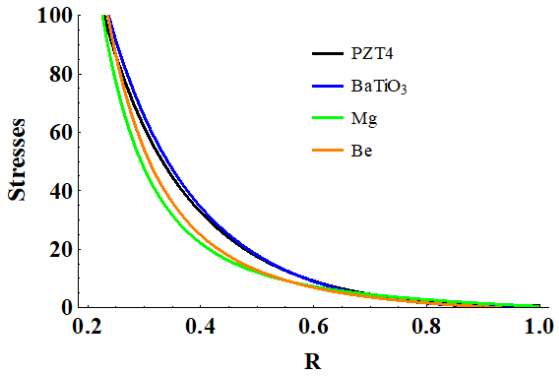

Figure 5. Graphs of creep stresses with $\theta = 0.5$, $\Omega = 10$ and measure n = 0.7.

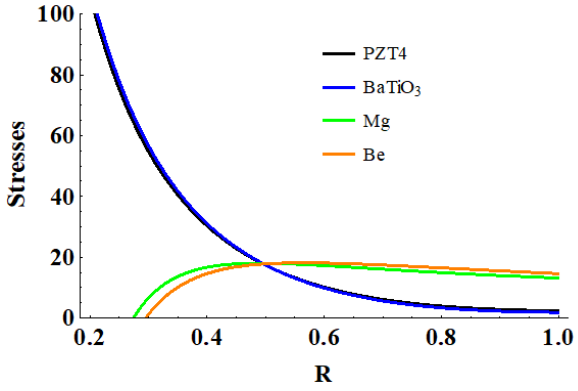

Figure 6. Graphs of creep stresses with $\theta = 0.5$, $\Omega = 10$ and measure n = 0.5.

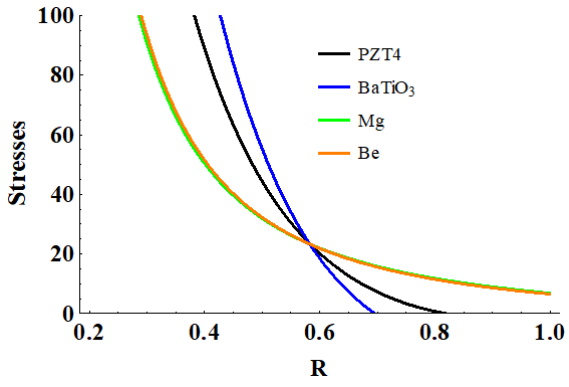

Figure 7. Graphs of creep stresses with $\theta = 0.5$, $\Omega = 20$ and measure n = 1.

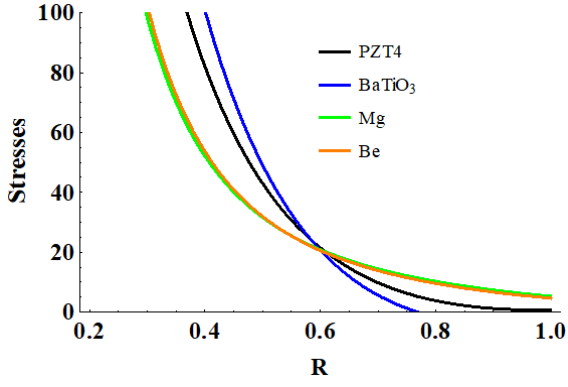

Figure 8. Graphs of creep stresses with $\theta = 0.5$, $\Omega = 20$ and measures n = 0.7.

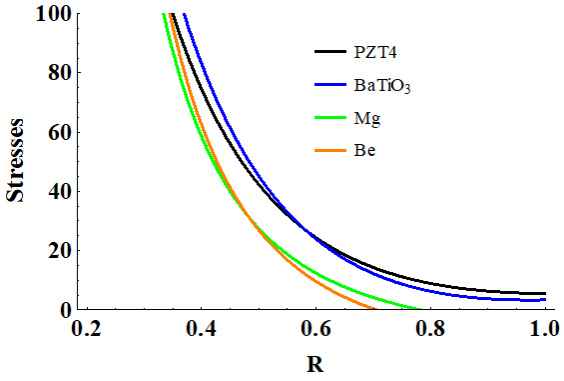

Figure 9. Graphs of creep stresses with $\theta = 0.5$, $\Omega = 20$ and measure n = 0.5.

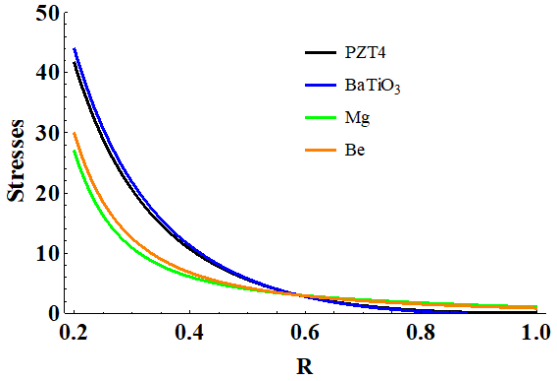

Figure 10. Graphs of creep stresses with $\theta = 0.3$, $\Omega = 5$ and measure n = 1.

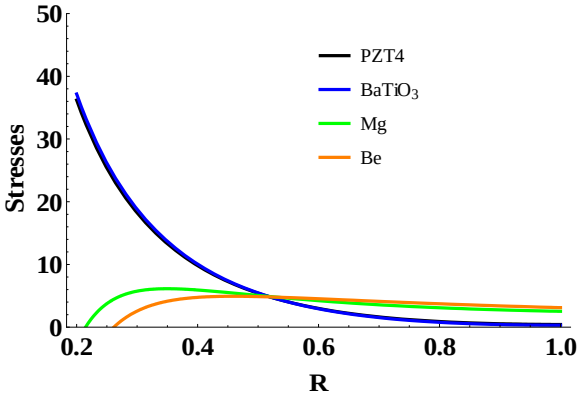

Figure 11. Graphs of creep stresses with $\theta = 0.3$, $\Omega = 5$ and measure n = 0.7.

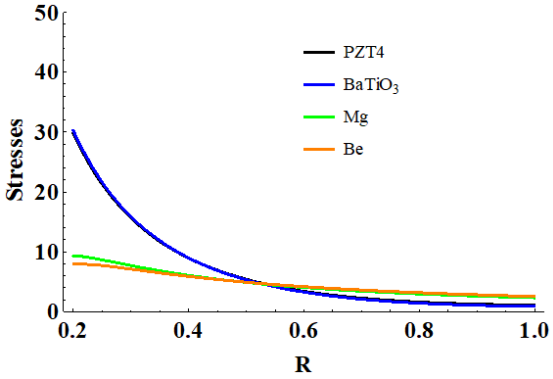

Figure 12. Graphs of creep stresses with θ = 0.3, Ω = 5 and measures n = 0.5.

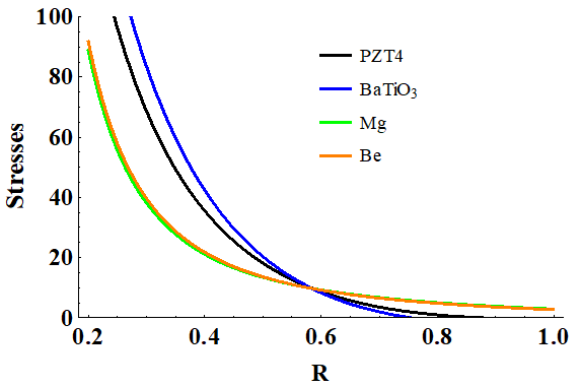

Figure 13. Graphs of creep stresses with $\theta = 0.3$, $\Omega = 10$ and measure n = 1.

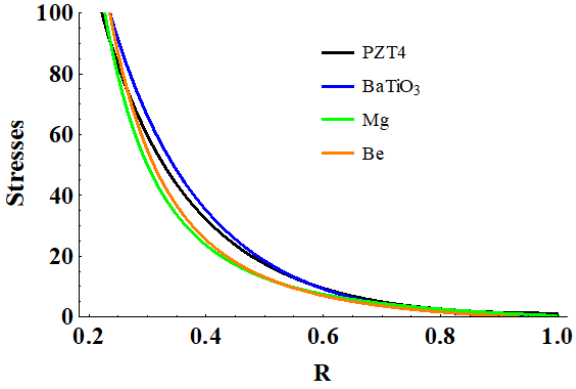

Figure 14. Graphs of creep stresses with $\theta = 0.3$, Ω =10 and measures n = 0.7.

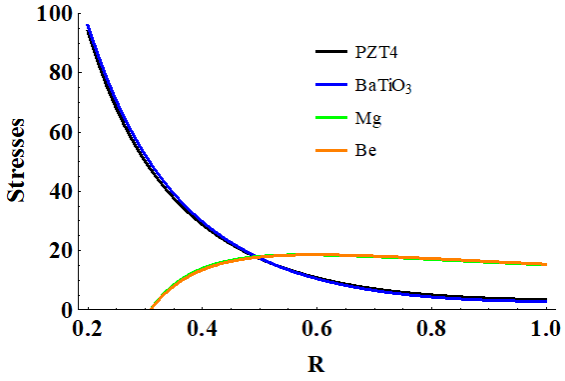

Figure 15. Graphs of creep stresses with $\theta = 0.3$, $\Omega = 10$ and measures $n = 0.5$

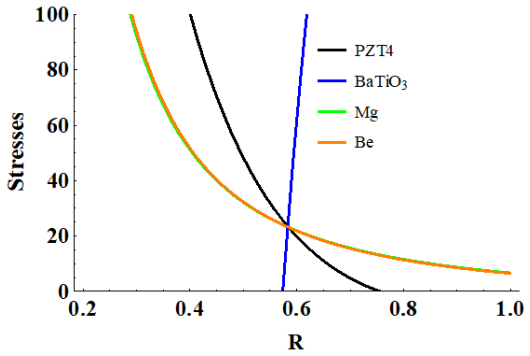

Figure 16. Graphs of creep stresses with $\theta = 0.3$, $\Omega = 20$ and measures $n = 1$.

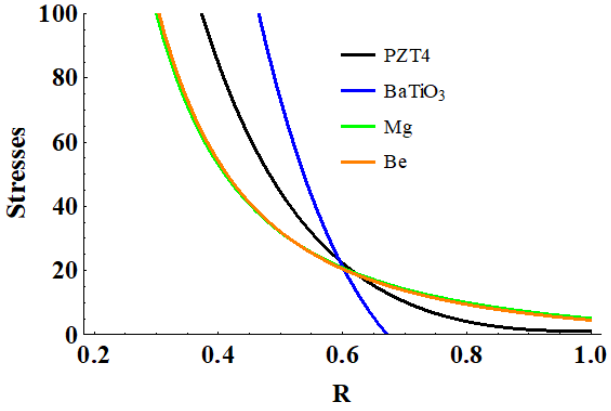

Figure 17. Graphs of creep stresses with $\theta = 0.3$, $\Omega = 20$ and measure n = 0.7.

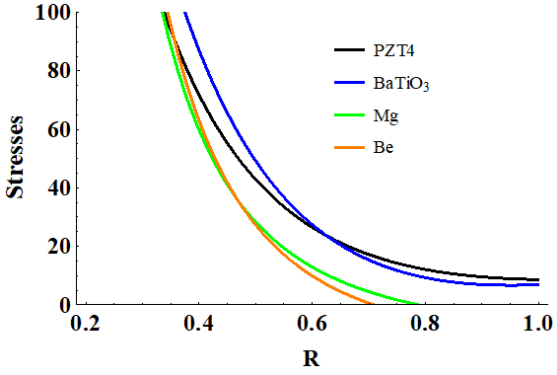

Figure 18. Graphs of creep stresses with θ = 0.3, Ω = 20 and measures n = 0.5.

Figure 1 represents the creep stresses for measures $n = 1, 0.5$ & 0.7, with angular velocity ($\Omega = 5$) and temperature $\theta = 0.5$. From **Figure 1** it is observed that creep stresses have maximum value at inner surface of the disc. When the radii ratio increases, these creep stresses become less in the case of a transversely isotropic disc (Magnesium and Beryl) and transversely isotropic piezoelectric (PZT4 and $BaTiO_3$) for linear measure. Also, the stresses are maximum in the case of transversely isotropic piezoelectric materials. From **Figures 2** and **3**, it is observed that stresses have less value for nonlinear measures $n = 0.5$ & 0.7 than linear measure in the case of all the considered transversely isotropic and piezoelectric materials.

From **Figures 4, 5,** and **6**, it is observed that creep stresses show an increase with the increasing value of angular velocity ($\Omega = 10$), creep stresses are minimum at the outer surface of the disc nearly equal to zero for transversely isotropic piezoelectric (PZT4 and $BaTiO_3$) with linear measure. The same pattern is shown by stresses for nonlinear measures (n = 0.7 and 0.5) as well. Stresses are higher at the inner surface and almost constant at the outer surface of the disc in transversely isotropic cases (Magnesium and Beryl). For measure ($n = 1$ & 0.7), the stresses coincide at the middle surface of the disc for all the materials under consideration. **Figures 7, 8** and **9** show the increase in creep stresses with the increasing value of angular

velocity ($\Omega = 20$). After comparing graphs for transversely isotropic and transversely isotropic piezoelectric materials, it was found that the value of creep stresses in transversely isotropic piezoelectric materials is higher than that of transversely isotropic materials. More specifically, $BaTiO_3$ has the highest creep stress of all the other materials.

Figures 10, 11 and **12** represent the creep stresses for measures $n = 1, 0.5$ & 0.7, with angular velocity ($\Omega = 5$) and temperature $\theta = 0.3$. It is observed that creep stresses have a maximum value at the inner surface of the disc and have an almost constant value at the outer surface of the disc for transversely isotropic as well as transversely isotropic piezoelectric materials with both linear and nonlinear measures. The value of creep stresses increases with increasing values of angular velocity ($\Omega = 10$), as observed in **Figures 13 to 15**. Stresses for transversely isotropic piezoelectric (PZT4 and $BaTiO_3$) have a minimum value at the middle surface and a maximum value at the internal surface. **Figures 16 to 18** show an increase in creep stresses with the increasing value of angular velocity ($\Omega = 20$).

5. Conclusion

We have considered the piezo-electric effect and transversely isotropic properties of creep material. The dynamical problem is then solved by using analytical techniques. The creep stress components have been solved numerically. The resulting quantities are depicted graphically to explore the effect of the piezoelectric parameter. On the basis of all the graphs and calculations, it is concluded that discs composed of transversely isotropic piezoelectric (PZT4 and $BaTiO_3$) materials are more stable than discs composed of transversely isotropic (Magnesium and Beryl) as creep stresses are maximum at the inner surface of the disc for transversely isotropic piezoelectric materials. Discs made of piezoelectric materials can bear more stresses, and the risk of fracture is less. So, these materials can be considered for design purposes. More specifically, discs composed of these types of materials can be utilized in actuators, sensors, transducers, etc. Further studies on circular discs made of transversely isotropic, orthotropic, and isotropic materials can be conducted for the improvisation of material structures used in various engineering applications.

Conflict of Interest

The authors have no potential conflict of interest.

Acknowledgments

The authors wish to extend their profound gratitude to the editor and reviewers for their invaluable assistance in enhancing and facilitating the publication of the manuscript.

References

Altenbach, H., & Skrzypek, J.J. (1999). *Creep and damage in materials and structures* (Vol. 399, pp. 348-348). Springer, Berlin.

Bagheri, R., Ayatollahi, M., & Mousavi, S.M. (2015). Analytical solution of multiple moving cracks in functionally graded piezoelectric strip. *Applied Mathematics and Mechanics*, *36*, 777-792.

Betton, J. (2005). *Creep mechanics*. Springer, Berlin.

Bhatnagar, N.S., & Arya, V.K. (1974). Large strain creep analysis of thick-walled cylinders. *International Journal of Non-Linear Mechanics*, *9*(2), 127-140.

Bhatnagar, N.S., & Gupta, S.K. (1969). Analysis of thick-walled orthotropic cylinder in the theory of creep. *Journal of the Physical Society of Japan*, *27*(6), 1655-1661.

Borah, B.N. (1971). On the yield condition and transition fields in elasto-plastic deformation of solids. *International Journal of Pure and Applied Mathematics*, *2*, 335-343.

Chand, S., Sood, S., Thakur, P., Gupta, K. (2023). Elastoplastic stress deformation in an annular disk made of isotropic material and subjected to uniform pressure. *Structural Integrity and Life*, *23*(1), 61-64.

Chandrasekharaiah, D.S. (1988). A generalized linear thermoelasticity theory for piezoelectric media. *Acta Mechanica*, *71*(1), 39-49.

Es-Saheb, M.H., & Fouad, Y. (2023). Creep analysis of rotating thick cylinders subjected to external and internal pressure: Analytical and numerical approach. *Applied Sciences*, *13*(21), 11652.

Fartash, A.H., Ayatollahi, M., & Bagheri, R. (2019). Transient response of dissimilar piezoelectric layers with multiple interacting interface cracks. *Applied Mathematical Modelling*, *66*, 508-526.

Hoseini, Z., Nejad1, M.Z., Niknejad, A., Ghannad, M. (2011). New exact solution for creep behaviour of rotating thick-walled cylinders. *Journal of Basic and Applied Scientific Research*, *1*(10), 1704-1708.

Kumar, A., & Ailawalia, P. (2019). Dynamic problem in piezo-electric microstretch thermoelastic medium under laser heat source. *Multidiscipline Modeling in Materials and Structures*, *15*(2), 473-491.

Matvienko, O., Daneyko, O., Valikhov, V., Platov, V., Zhukov, I., & Vorozhtsov, A. (2023). Elastoplastic deformation of rotating disk made of aluminum dispersion-hardened alloys. *Metals*, *13*(6), 1028.

Mindlin, R.D. (1974). Equations of high frequency vibrations of thermopiezoelectric crystal plates. *International Journal of Solids and Structures*, *10*(6), 625-637.

Penny, R.K., Marriott, R.K. (1995). *Design of creep*. Mc-Grew Hill, Springer.

Rimrott, F.P.J. (1959). Creep of thick-walled tubes under internal pressure considering large strains. *Journal of Applied Mechanics, Transactions of the ASME*, *1*, 271-275.

Saadatfar, M., Babazadeh, M.A., & Babaelahi, M. (2024). Stress and deformation of a functionally graded piezoelectric rotating disk with variable thickness subjected to magneto-thermo-mechanical loads including convection and radiation heat transfer. *International Journal of Applied Mechanics*, *16*(1), 2450002.

Sharma, R. (2019). Elastic-plastic stresses in a thin rotating disk of functionally graded material with exponentially varying thickness under internal pressure. *Structural Integrity and Life*, *19*(3), 185-194.

Sharma, R. (2023) Evaluation of thermal elastic-plastic stresses in transversely isotropic disk made of piezoelectric material with variable thickness and variable density subjected to internal pressure. *Structural Integrity and Life*, *23*(2), 205-212.

Sharma, R., Sahni, M. (2020). Analysis of creep stresses in thin rotating disc composed of piezoelectric material. *Structural Integrity and Life*, *20*, S45-S49.

Sharma, S., & Yadav, S. (2019). Numerical solution of thermal elastic-plastic functionally graded thin rotating disk with exponentially variable thickness and variable density. *Thermal Science*, *23*(1), 125-136.

Sharma, S., Sahni, M., & Sharma, R. (2017). Creep deformation of a non-homogeneous thin rotating disk of exponentially varying thickness with internal pressure. In *AIP Conference Proceedings* (Vol. 1897, No. 1). AIP Publishing. Uttar Pradesh, India.

Sharma, S., Sharma, R., & Panchal, R. (2018). Creep transition in transversely isotropic composite circular cylinder subjected to internal pressure. *International Journal of Pure and Applied Mathematics*, *120*(1), 87-96.

Singh, R., Saxena, R., Khanna, K., & Gupta, V. (2020). Creep response of rotating composite discs having exponential hyperbolic linear and constant thickness profiles. *Defence Science Journal*, *70*(3), 292-298.

Singh, T., & Gupta, V.K. (2009). Effect of material parameters on steady state creep in a thick composite cylinder subjected to internal pressure. *The Journal of Engineering Research*, *6*(2), 20-32.

Tauchert, T.R., (1992). Piezo thermoelastic behaviour of plate of crystal class 6mm a laminated plate. *Journal of Thermal Stresses*, *15*, 25-37.

Temesgen, A.G., Singh, S.B., & Pankaj, T. (2020). Modeling of creep deformation of a transversely isotropic rotating disc with a shaft having variable density and subjected to a thermal gradient. *Thermal Science and Engineering Progress*, *20*, 100745.

Thakur, P., & Sethi, M. (2020). Creep deformation and stress analysis in a transversely material disk subjected to rigid shaft. *Mathematics and Mechanics of Solids*, *25*(1), 17-25.

Yang, Y., Li, Y., Pan, J., Luo, T., & Lu, Z. (2021). Experimental study on creep behavior and crack evolution of stratified structural sandstone under segmental constant load. *Geofluids*, *2021*, 1-29.

Zhou, H., Han, K., Elmaimouni, L., Wang, X., & Yu, J. (2024). Double Legendre polynomial quadrature-free method for axisymmetric vibration of functionally graded piezoelectric circular plates. *Journal of Vibration and Control*, *30*(3-4), 598-615.